pounds[8-11,13-15,17] and the experimental procedures for obtaining the ^{95}Mo NMR spectra[18] have been described.

It has been previously established that $[(XCu)MoS_4]^{2-}$ complexes adopt structure **1** (see Table I) in the solid state.[8,9,11,13] In solution, such complexes give relatively sharp ^{95}Mo NMR signals near 1900 ppm with line widths of ~50 Hz.[9,11,13] $[(XCu)_2MoS_4]^{2-}$ complexes (structure **2**)[11,13] have ^{95}Mo NMR resonances in the 1600–1700 ppm range with line widths that are 200 Hz or greater.[11,13]

Here, we present the first ^{95}Mo NMR data for $[(XCu)_3MoS_4]^{2-}$ and $[(XCu)_4MoS_4]^{2-}$ clusters. The former adopt structure **3**[14,15] in the solid state and in solution show a chemical shift range of 1230–1280 ppm with line widths of ~200 Hz. The $[(XCu)_4MoS_4]^{2-}$ ions (**4**)[10] have ^{95}Mo NMR resonances near 900 ppm, and the lines are substantially broader (~1400 Hz) than any of the other Cu–Mo–S species.

The data in the table show that the molybdenum chemical shift decreases monotonically as additional CuX units are bound to the $[MoS_4]^{2-}$ core of the clusters. Thus, the molybdenum chemical shift of a $[(XCu)_nMoS_4]^{2-}$ cluster provides a direct measure of the number of CuX units in the cluster. Each successive addition of a CuX moiety to the $[MoS_4]^{2-}$ core results in a decrease in the chemical shift of the molybdenum nucleus by 200–400 ppm. smaller variations in the molybdenum chemical shift result from changing the nature of the X ligand attached to the Cu atom. The general variation of the shielding of the molybdenum nucleus with the X substituent on Cu seems to be SPh < I < Br < Cl ~ CN, although the data do not permit direct comparison of the effects of I and SPh.

The table also presents ^{95}Mo data for some Cu–Mo–S clusters derived from the $[MoOS_3]^{2-}$ and $[MoO_2S_2]^{2-}$ anions. Direct comparison of the ^{95}Mo chemical shifts of $[(PhSCu)MoS_4]^{2-}$ and $[(PhSCu)MoO_2S_2]^{2-}$ shows that the molybdenum nucleus is ~1300 ppm more shielded in $[(PhSCu)MoO_2S_2]^{2-}$. This shielding difference is very similar to that in the parent anions where $[MoO_2S_2]^{2-}$ is ~1150 ppm more shielded than $[MoS_4]^{2-}$.[13,19] The pair $[(ClCu)_3MoOS_3]^{2-}$ and $[(ClCu)_3MoS_4]^{2-}$ exhibits increased shielding of ~760 ppm for the oxo-containing complex. The line widths of the latter pair are also dramatically different, presumably reflecting the different structures (**7**[20] and **3**,[14,21] respectively) adopted by the two ions. Similar shielding differences occur for the pair $[(PhSCu)_2MoOS_3]^{2-}$ and $[(PhSCu)_2MoS_4]^{2-}$ (808 ppm) and for the pair $[(NCCu)MoOS_3]^{2-}$ and $[(NCCu)MoS_4]^{2-}$ (665 ppm[13]).

The ^{95}Mo NMR resonances of the $[(XCu)_nMoS_4]^{2-}$ anions are all much broader than those for $[MoS_4]^{2-}$. The presence of quadrupolar copper nuclei and the increased molecular mass of Cu–Mo–S clusters can both contribute to line broadening. However, the data in the table show that there is no simple correlation between the number of copper atoms in the complexes (n) and the line width. The complexes with $n = 2$ and 3 have similar line widths (170–600 Hz) that are much larger than complexes with $n = 1$ and much smaller than complexes with $n = 4$.

In summary, this work clearly demonstrates that ^{95}Mo NMR chemical shifts can be used to identify various $[(XCu)_nMoS_4]^{2-}$ ions in solution and hence is a simple direct probe for determining the CuX:MoS_4 ratio for unknown complexes in solution. This research also provides good evidence that the Cu–Mo–S clusters do not dissociate in solution because each complex gives only one ^{95}Mo resonance.

Related Cu(I) complexes are formed by $[MoO_ySS_{4-y}]$ (y = 0–2) anions.[2] The nature of the S–Mo–O core (i.e., the value of y) for such species is readily established from their vibrational and electronic spectra.[11,16] The present work has established that the ^{95}Mo chemical shifts of $[(XCu)_nMoO_yS_{4-y}]^{2-}$ species clearly identify the value of n for a given value of y. Therefore, on the basis of the ^{95}Mo NMR spectrum and the vibrational and/or electronic spectra, it is possible to determine both y and n for such complexes. The ability to distinguish and identify Cu–Mo–S clusters in solution should be of considerable value in further developing the chemistry of such systems. Also, there now exists the exciting prospect of using a combination of ^{95}Mo NMR and other spectroscopies to characterize the Cu–Mo–S species that may be present when molybdenum induces copper deficiency in ruminants.[3,4] Such studies could be further enhanced by using ^{95}Mo-enriched samples to increase the sensitivity of the ^{95}Mo NMR measurements.

Acknowledgment. Support of portions of this work by the U.S. Department of Agriculture (Grant No. 81-CRCR-1-0626) and by the North Atlantic Treaty Organization is gratefully acknowledged. J.R.N. thanks the SERC for a studentship. We thank Dr. K. E. Christensen for assistance with the NMR measurements and Dr. A. G. Wedd for a preprint of ref 13.

Registry No. **2**·2PPh_4 (X = Br), 92787-47-8; **2**·2PPh_4 (X = Cl), 92787-49-0; **3**·2PPh_4 (X = I), 92787-51-4; **3**·2PPh_4 (X = Br), 92787-53-6; **3**·2PPh_4 (X = I), 85752-65-4; **4**·2PPh_4 (X = Br), 88433-65-2; **4**·2PPh_4 (X = Cl), 88433-62-9; **6**·PPh_4 (X = SPh), 92787-55-8; **7**·2PPh_4 (X = Cl), 86430-80-0; **8**·2PPh_4 (X = Cl), 92787-57-0; ^{95}Mo, 14392-17-7.

(17) Nicholson, J. R.; Boyde, S.; Garner, C. D.; Clegg, W., submitted for publication.
(18) Minelli, M.; Bell, A.; Enemark, J. H.; Walton, R. A. *J. Organomet. Chem.*, in press.
(19) Lutz, O.; Nolle, A.; Kroneck, P. *Z Naturforsch., A* **1976**, *31A*, 454; **1977**, *32A*, 505.
(20) Clegg, W.; Garner, C. D.; Nicholson, J. R.; Raithby, P. R. *Acta Crystallogr., Sect. C: Cryst. Struct. Commun.* **1983**, *C39*, 552.
(21) Müller, A.; Schimanski, U.; Schimanski, J. *Inorg. Chim. Acta* **1983**, *76*, L245.

Contribution from the Departments of Chemistry, University of Hong Kong, Hong Kong, and The Chinese University of Hong Kong, Shatin, New Territories, Hong Kong, and Contribution No. 7073 from Arthur Amos Noyes Laboratory, California Institute of Technology, Pasadena, California 91125

A Dimeric Platinum(III) System Containing a Long Metal–Metal Bond. Crystal Structure of $K_4[Pt_2(P_2O_5H_2)_4CH_3I]\cdot 2H_2O$

Chi-Ming Che,*[1a] Thomas C. W. Mak,*[1b] and Harry B. Gray[1c]

Received March 6, 1984

Earlier we found that binuclear platinum(III) species can be obtained readily by oxidative addition of halogens or methyl iodide to $[Pt_2(pop)_4]^{4-}$ (pop = $P_2O_5H_2^{2-}$).[2] Though fragmentation of alkyl halides in two-center oxidative additions has been observed before,[3] relatively few structural studies on the adducts have been performed. Here we wish to report the structure of $[Pt_2(pop)_4CH_3I]^{4-}$, which was obtained through the reaction of $[Pt_2(pop)_4]^{4-}$ with CH_3I; the structural results

(1) (a) University of Hong Kong. (b) The Chinese University of Hong Kong. (c) California Institute of Technology.
(2) Che, C.-M.; Schaefer, W. P.; Gray, H. B.; Dickson, M. K.; Stein, P. B.; Roundhill, D. M. *J. Am. Chem. Soc.* **1982**, *104*, 4253.
(3) See, for example: (a) Lewis, N. S.; Mann, K. R.; Gordon, J. G., II; Gray, H. B. *J. Am. Chem. Soc.* **1976**, *98*, 7461. (b) Coleman, A. W.; Atwood, J. L. *J. Am. Chem. Soc.* **1982**, *104*, 922.

0020-1669/84/1323-4386$01.50/0

Table I. Data Collection and Processing Parameters

mol formula	$K_4[Pt_2(P_2O_5H_2)_4CH_3I]\cdot 2H_2O$
mol wt	1300.38
cell constants	$a = 9.475$ (3) Å, $c = 15.786$ (7) Å, $V =$ 1417 (1) Å^3, $Z = 2$
density (flotation in $CH_2I_2/BrCH_2CH_2Br$)	2.97 g cm^{-3}
density (calcd)	3.048 g cm^{-3}
space group	$I4/mmm$ (No. 139)
abs coeff	121.58 cm^{-1}
mean μr	1.0
transmission factors	0.073–0.137
scan type and speed	ω–2θ; 0.99–14.65° min^{-1}
scan range	1° below $K\alpha_1$ to 1° above $K\alpha_2$
bkgd	stationary counts for half of the scan time at each end of scan
collcn range	hkl; $2\theta_{max} = 75°$
no. of unique data measd	1079
no. of obsd data with $\|F\| > 3\sigma(\|F\|)$, n	961
no. of variables, p	39
extinction param ϵ	$[3.8\ (8)] \times 10^{-7}$
$R_F = \Sigma\|\|F_o\| - \|F_c\|\|/\Sigma\|F_o\|$	0.037
weighting scheme	$w = [\sigma^2(\|F_o\|) + 0.00005\|F_o\|^2]^{-1}$
$R_G = [\Sigma w(\|F_o\| - \|F_c\|)^2/\Sigma w\|F_o\|^2]^{1/2}$	0.047
$S = [\Sigma w(\|F_o\| - \|F_c\|)^2/(n-p)]^{1/2}$	2.584

indicate that there is substantial mixing among the Pt–CH_3, Pt–I, and Pt–Pt bonds.

Experimental Section

Preparation of $K_4[Pt_2(pop)_4CH_3I]\cdot 2H_2O$. A 0.4-g sample of $K_4[Pt_2(pop)_4]$[4] in 10 mL of H_2O was treated with excess CH_3I (3 mL), and the resulting solution was left in open air for 1 day. A yellowish brown microcrystalline solid (which shows a green metallic lustre in several preparations) was obtained. This was then filtered and washed with ethanol and ice-cooled water. The solid may be recrystallized in water although sample decomposition was sometimes observed. Anal. Calcd for $K_4[Pt_2(pop)_4CH_3I]\cdot 2H_2O$: C, 0.92; P, 19.05; I, 9.76. Found: C, 0.85; P, 19.00; I, 9.76. IR spectrum, $\nu(CH_3)$: 2930 cm^{-1} (KBr pellet). UV–vis spectrum in H_2O, λ_{max}/nm (log ϵ): 346 (4.47), 325, sh (4.11), 278 (3.96). Detailed NMR spectroscopic characterization of $K_2[Pt_2(pop)_4CH_3I]$ has been reported previously.[2]

Crystallographic Studies

The sample studied consisted of a mixture of two crystalline forms: yelllow crystals and a much larger quantity of green lustrous crystals. The UV–vis spectrum of the yellow form is essentially the same as reported above. The green form, upon dissolution in water, showed an intense UV–vis absorption band at 367 nm, indicating the presence of $K_4[Pt_2(pop)_4]$. Only the yellow crystals yielded good diffraction data. A selected crystal block (0.20 × 0.15 × 0.10 mm) was optically centered on a Nicolet R3m computer-controlled four-circle diffractometer. Determinations of the crystal system, Laue class, orientation matrix, and accurate unit cell dimensions were performed according to established procedures.[5] Intensity date were collected (details summarized in Table I) at an ambient laboratory temperature of 22 ± 1 °C by using graphite-monochromatized Mo $K\alpha$ radiation (λ = 0.71069 Å). The crystal remained stable throughout the diffraction experiment, as three standard reflections monitored every 125 data measurements showed only random deviations within ±1% of their mean values. Absorption correction was applied by using an empirical method based on a pseudoellipsoidal treatment of azimuthal (ψ) scans of selected strong reflections.[6] Redundant and equivalent reflection data were averaged and converted to unscaled $|F_o|$ values following corrections for Lorentz and polarization factors. Statistical distributions of the normalized structure factors $|E|$ were consistent with those expected for a centrosymmetric space group.

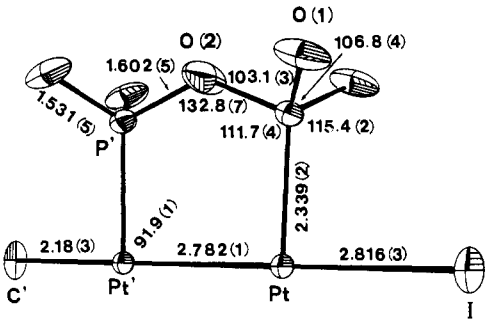

Figure 1. Structural features of the $[Pt_2(pop)_4CH_3I]^{4-}$ anion. For clarity, disorder of the iodide and methyl groups is not shown, and only one bridging diphosphite ligand is illustrated. The primed atoms are generated from the unprimed ones by the symmetry transformation $(x, y, -z)$.

A sharpened Patterson function yielded the positions of the Pt and I atoms, and it soon became apparent that $[Pt_2(pop)_4CH_3I]^{4-}$ occupies a special position of site symmetry $4/mmm$ in space group $I4/mmm$, with CH_3 and I each disordered over two positions at both ends of the binuclear anion. The remaining K, P, O, and Ow (water) atoms were located from subsequent difference Fourier syntheses, and the peak heights clearly indicated half site occupancy for K(2) and Ow. The H atoms were not located, and all non-H atoms except C were refined anisotropically. The final difference map showed residual extrema from 2.08 to −2.28 e Å^{-3}, with the two highest peaks lying in the neighborhood of the I and Pt atoms.

All computations were performed on a Data General Corporation Nova 3/12 minicomputer with the SHELXTL program package.[7] Analytical expressions of neutral-atom scattering factors were employed, and anomalous dispersion corrections were incorporated.[8] Blocked-cascade least-squares refinement of 39 parameters, including an empirical isotropic extinction parameter[9] ϵ in the expression $F_{cor} = F_c/[1 + \epsilon F_c^2/\sin(2\theta)]^{1/4}$, converged to the R indices shown in Table I.

Results and Discussion

Table II lists the final atomic coordinates. Selected bond distances and bond angles are given in Figure 1. Thermal parameters and tables of structure factors are available as supplementary material, as specified in the last paragraph of this paper.

The salient feature of the present structure is the Pt–Pt bond length of 2.782 (1) Å, which is shorter than the Pt–Pt distance of 2.925 (1) Å[10] in the unoxidized $[Pt_2(pop)_4]^{4-}$ species but considerably exceeds those in the related $[Pt_2(pop)_4Cl_2]^{4-}$ unit [2.695 (1) Å],[10] as well as in other discrete binuclear Pt(III) species such as $[Pt_2(SO_4)_4(H_2O)_2]^{2-}$ [2.466 (?) Å],[11] $[Pt_2(SO_4)_4(OSMe)_2]^{2-}$ [2.471 (1) Å],[12] and $[Pt_2(HPO_4)_4(H_2O)_2]^{2-}$ [2.486 (2) Å].[13] Interpretation of the $[Pt_2(pop)_4CH_3I]^{4-}$ species as a singly bonded Pt(III)–Pt(III) system is supported by its observed diamagnetism.[14] In accordance with expectation, the present Pt–Pt distance is slightly shorter than that [2.793 (1) Å][10] in the linear-chain semiconductor $K_4[Pt_2(pop)_4Br]\cdot 2H_2O$, which has a formal oxidation state of +2.5.

Variation of the Pt–Pt distance in discrete binuclear Pt_2L_4 systems has previously been attributed to the constraining

(4) Che, C.-M.; Butler, L. G.; Gray, H. B., results to be published.
(5) Sparks, R. A. In "Crystallographic Computing Techniques"; Ahmed, F. R.; Ed.; Munksgaard: Copenhagen, 1976; p 452.
(6) (a) Kopfmann, G.; Huber, R. *Acta Crystallogr., Sect. A* **1968**, *A24*, 348. (b) North, A. C. T.; Phillips, D. C.; Mathews, F. S. *Ibid.* **1968**, *A24*, 351.
(7) Sheldrick, G. M. In "Computational Crystallography"; Sayre, D., Ed.; Oxford University Press: New York, 1982; p 506.
(8) "International Tables for X-ray Crystallography"; Kynoch Press: Birmingham, England, 1973; Vol. IV, pp 99, 149.
(9) Larson, A. C. *Acta Crystallogr.* **1967**, *23*, 664.
(10) Che, C.-M.; Herbstein, F. H.; Schaefer, W. P.; Marsh, R. E.; Gray, H. B. *J. Am. Chem. Soc.* **1983**, *105*, 4604.
(11) Muraveiskaya, G. S.; Kukina, G. A.; Orlova, V. S.; Evstaf'eva, O. N.; Porai-Koshits, M. A. *Dokl. Akad. Nauk SSSR* **1976**, *226*, 596.
(12) Cotton, F. A.; Falvello, L. R.; Han, S. *Inorg. Chem.* **1982**, *21*, 2889.
(13) Cotton, F. A.; Falvello, L. R.; Han, S. *Inorg. Chem.* **1982**, *21*, 1709.
(14) Solutions of $[Pt_2(pop)_4CH_3I]^{4-}$ gave well-resolved $^{13}C\{^1H\}$ NMR spectra.
(15) Bellitto, C.; Flamino, A.; Gastoldi, L.; Scaramuzza, L. *Acta Crystallogr., Sect. A* **1981**, *A37*, C172.

Table II. Atomic Coordinates (×10⁵ for Pt, I, and P; ×10⁴ for K, O, and C) and Equivalent Isotropic Temperature Factors[a] (Å² × 10⁴ for Pt, I, and P; Å² × 10³ for K, O, and C)

atom	Wyckoff position	site symm	*x*	*y*	*z*	U_{eq}
Pt	4(e)	4*mm*	0	0	8811 (4)	176 (1)
I	4(e)	4*mm*	0	0	26647 (16)	452 (6)[b]
P	16(n)	*m*	0	24670 (19)	9302 (14)	248 (5)
O(1)	32(o)	1	1297 (4)	3138 (5)	1345 (4)	50 (2)
O(2)	8(i)	*mm*	0	3144 (12)	0	103 (7)
C	4(e)	4*mm*	0	0	2260 (24)	31 (6)[b,c]
K(1)	4(d)	$\bar{4}m2$	0	5000	2500	36 (1)
K(2)	8(j)	*mm*	2600 (7)	5000	0	41 (2)[b]
Ow	8(j)	*mm*	5000	3210 (23)	0	61 (9)[b]

[a] Calculated as one-third of the trace of the orthogonalized U_{ij} matrix. [b] Half site occupancy. [c] Varied isotropically.

effect of the bridging ligand L.[10] However, the observed lengthening (ca. 0.09 Å) of the Pt–Pt distance in $[Pt_2(pop)_4CH_3I]^{4-}$ relative to that in $[Pt_2(pop)_4Cl_2]^{4-}$ clearly indicates that a strong trans influence is exerted by the methyl and iodide ligands. In accordance with this, the $E(d\sigma \rightarrow d\sigma^*)$ transition has been found to be substantially red shifted in going from $[Pt_2(pop)_4Cl_2]^{4-}$ to $[Pt_2(pop)_4CH_3I]^{4-}$.

The Pt-I bond distance in the present complex [2.816(3) Å] lies between that of a Pt–I single bond (ca. 2.64–2.68 Å)[16-18] and those observed in $[Pt_2(S_2CMe)_4I]$ [2.975 (2) and 2.981 (3) Å].[15] It is, in fact, comparable to the shorter of the two alternating metal–halide distances along the chain in such Wolfram's salt analogous as $[Pt(dapn)_2][Pt(dapn)_2I_2](ClO_4)_4$ [2.791 (8) and 3.036 (8) Å][19] and $[Pt(dapn)_2][Pt(dapn)_2I_2]I_4$ [2.815 (2) and 2.995 (2) Å],[20] where dapn stands for 1,2-diaminopropane. The Pt–C bond of 2.18 (3) Å is also significantly longer than most Pt^{II}–C σ-bonds (ca. 2.08 Å[21]) and compares well with the Pt^{IV}–C distance of 2.15 (1) Å in $PtI_2(CH_2)_4(PMe_2Ph)_2$.[8] The observed lengthening of the Pt–CH_3, Pt–I, and Pt–Pt bonds in $[Pt_2(pop)_4CH_3I]^{4-}$ is consistent with axial σ electronic delocalization and suggests further that the Pt^{III} species will undergo reductive elimination relatively easily.

The pronounced anisotropic thermal motion of O(1) and O(2) (Figure 1) is probably more representative of minor positional disorder imposed by the required 4/*mmm* symmetry of $[Pt_2(pop)_4CH_3I]^{4-}$ anion rather than a large vibrational effect. Allowing for the statistical equivalence of the P=O and P—OH groups, the measured dimensions of the diphosphite ligand and the Pt–P distance (Figure 1) are in reasonable agreement with those observed in the series $[Pt_2(pop)_4]^{4-}$, $[Pt_2(pop)_4Br]^{4-}$, and $[Pt_2(pop)_4Cl_2]^{4-}$.[10,22]

The potassium ions, which occupy two different special positions iin the unit cell, play a critical role in consolidating the crystal packing through ionic interactions with both the diphosphite and water oxygen atoms. Atom K(1) is located at a site of symmetry $\bar{4}m2$, being surrounded by eight symmetry-equivalent O(1) atoms arranged in two rectangles normal to the *c* axis [K(1)···O(1) = 2.819(5) Å].[23] Atom K(2) half-occupies a site of symmetry *mm*; it is also eight-coordinate, but the primary coordination sphere is less regular and comprises four interactions with O(1) at 3.024 (6) Å, two with O(2) at 3.027 (8) Å, and two with Ow at 2.837 (14) Å.[24] Unlike the water molecule in $K_4[Pt_2(pop)_4Cl_2]\cdot 2H_2O$,[10] which is hydrogen bonded to diphosphite ions, the 2-fold disordered Ow atom in $K_4[Pt_2(pop)_4CH_3I]\cdot 2H_2O$ serves only as a bridging ligand between two symmetry-related K(2) atoms.

It is of interest to compare the crystal structures of the series of binuclear platinum diphosphite complexes $K_4[Pt_2(pop)_4]\cdot 2H_2O$, $K_4[Pt_2(pop)_4Br]\cdot 2H_2O$, $K_4[Pt_2(pop)_4Cl_2]\cdot 2H_2O$, and $K_4[Pt_2(pop)_4CH_3I]\cdot 2H_2O$. In the first two complexes (same space group, *P4/mbm*), the roughly cylindrical $Pt_2(pop)_4$ "barrels" stack in columns parallel to the *c* axis, whereas no such end-to-end stacking occurs in the dichloro complex (space group $P\bar{1}$). In $K_4[Pt_2(pop)_4CH_3I]\cdot 2H_2O$, the noninteracting $Pt_2(pop)_4$ barrels are arranged in columns along the *c* direction, with a much increased interbarrel gap necessitated by the *I* lattice centering. It is noteworthy that the *a* axis of $K_4[Pt_2(pop)_4CH_3I]\cdot 2H_2O$ is approximately equal to half of the face diagonal of the base of the unit cell in either $K_4[Pt_2(pop)_4]\cdot 2H_2O$ or $K_4[Pt_2(pop)_4Br]\cdot 2H_2O$ (see Figure 1 of ref 10), indicating very similar lateral packing of the columns in the three tetragonal crystalline compounds.

Acknowledgment. C.-M.C. thanks the Committee on Research and Conference Grants of the University of Hong Kong for support. Research at Caltech was supported by National Science Foundation Grant CHE81-20419.

Registry No. $K_4[Pt_2(pop)_4CH_3I]\cdot 2H_2O$, 93134-17-9; $K_4[Pt_2(pop)_4]$, 82135-51-1; CH_3I, 74-88-4; $K_4[Pt_2(pop)_4CH_3I]$, 82135-52-2; Pt, 7440-06-4.

Supplementary Material Available: Listings of structure factors (Table III) and anisotropic thermal parameters (Table IV) (7 pages). Ordering information is given on any current masthead page.

(16) Freckmann, B.; Tebbe, K.-F. *Acta Crystallog., Sect. B* **1981**, *B37*, 1520.
(17) Thiele, G.; Wagner, D. *Z. Anorg. Allg. Chem.* **1978**, *446*, 126.
(18) Cheetham, A. K.; Puddephatt, R. J.; Zalkin, A.; Templeton, D. H.; Templeton, L. K. *Inorg. Chem.* **1976**, *15*, 2997.
(19) Endres, H.; Keller, H. J.; Martin, R.; Gung, H. N.; Traeger, U. *Acta Crystallogr., Sect. B* **1979**, *B35*, 1885.
(20) Endres, H.; Keller, H. J.; Martin, R.; Traeger, U.; Novotny, M. *Acta Crystallogr., Sect. B* **1980**, *B36*, 35.
(21) Bardi, Piazzesi, A. M. *Inorg. Chim. Acta* **1981**, *47*, 249.
(22) Pinto, M. A. F. D. R.; Sadler, P. J.; Neidle, S.; Sanderson, M. R.; Subbiah, A.; Kuroda, R. *J. Chem. Soc., Chem. Commun.* **1980**, *13*.
(23) Symmetry-generated O(1) positions at (x, y, z), $(-x, y, z)$, $(x, 1-y, z)$, $(-x, 1-y, z)$, $(^1/_2-y, ^1/_2-x, ^1/_2-z)$, $(^{-1}/_2+y, ^1/_2-x, ^1/_2-z)$, $(^1/_2-y, ^1/_2+x, ^1/_2-z)$, and $(^{-1}/_2+y, ^1/_2+x, ^1/_2-z)$.
(24) Symmetry-generated O(1) positions at (x, y, z), $(x, y, -z)$, $(x, 1-y, z)$, and $(x, 1-y, -z)$; O(2) positions at (x, y, z) and $(x, 1-y, z)$; Ow positions at (x, y, z) and $(x, 1-y, z)$.

Contribution from the Department of Chemistry, Faculty of Science and Technology, Kinki University, Kowakae, Higashi-Osaka, 577 Japan

^{63}Cu NMR Studies of Copper(I) Complexes. Relationship between ^{63}Cu Chemical Shift and Metal–Ligand Binding

Susumu Kitagawa* and Megumu Munakata

Received January 5, 1984

Copper(I) complexes, which occur naturally in the active sites of copper proteins,[1] and are utilized in organic synthesis

